

STRUCTURAL TRANSFORMATION OF HCP METALLIC NANOWIRE USING CLERI-ROSATO POTENTIAL

M.M. Aish*

Physics Department, Faculty of Science, Menoufia University, 32511 Shebin Elkom, Menofia, Egypt

*e-mail: mohamedeash2@yahoo.com

Abstract. Sub-atomic Dynamic simulations have been carried out on some single-crystal hexagonal metals, HCP nanowires (Cd, Co, Mg, Ti, and Zr) upon application of uniaxial tension with a speed of 20 m/s and to investigate the nature of deformation and fracture. The deformation corresponds to the direction $\langle 0001 \rangle$ plane. A many-body interatomic potential for HCP nanowires within the second-moment approximation of the tight-binding model (the Cleri-Rosato potentials) was employed to carry out three dimensional MD simulations. A computer experiment is performed at a temperature 300K. The stored energy diagrams obtained at various time by the MD simulations of the tensile specimens of these metallic nanowires show a rapid increase in stress up to a maximum followed by a gradual drop to zero when the specimen fails by ductile fracture. The feature of deformation energy can be divided into three regions: quasi-elastic, plastic and failure. The nature of deformation, slipping, twinning and necking were studied. Stress decreased with increasing volume and the breaking position increases. The results showed that breaking position depended on the nanowire length. From this, it appears that Cleri-Rosato potentials make good represent for the deformation behavior of HCP metallic nanowires.

Keywords: molecular dynamics, uniaxial tension, Cleri-Rosato, nanowires, tight-binding and failure

1. Introduction

Physical and mechanical properties of the substances in condensed matter physics depended on size and structure: With decreasing size of the elementary particles that make up the material, increase the strength and feature of plasticity changes were studied in [1]. In the past ten years, special attention has been given to the studied the properties of metallic nanowires and nanofilms and another nano-objects [2]. Nanowires referred to as materials, which are in the cross-section size is not more than 100 nm and significantly extended in length. Other important systems include metallic nanostructured and alloys, which have unique properties, and can be used as structural or functional materials [1]. First of all, this is due to the fact that they have been studied and has accumulated extensive experimental data. Of particular interest in terms of the choice of the object of study are those metals and alloys, in which, first, has the longest period of nanosize. Second, the weak-stable to external influences (temperature, load, doping and so on.). Third, there is a range of structural states near the boundary of stability loss, and these states are in equilibrium or near-equilibrium.

These requirements are responsible, in particular, ordered alloys and intermetallic compounds which contain long periodic structure (LPS). From the normal ordered systems with a simple superstructure, they differ in that the alloys of this class ordered arrangement of atoms periodically or quasi-periodically broken antiphase boundaries (APB). Normally, in ordered alloys and intermetallic compounds APB energetically favorable, however, in

systems with long-period equilibrium nanostructure APB are elements of the structure. Given that the mechanisms of structural-energy transformations at various load conditions, in particular uniaxial strain, help to explain the abnormal strength properties of long-period metal alloys (LPMA), ie the properties of LPMR resist destruction and irreversible change in the shape, the task of studying the mechanisms of structural-energy transformations occurring during high uniaxial strain tension of HCP metallic (Cd, Co, Mg, Ti, and Zr) nanowires, containing LPS. Because of the strong anisotropy of the structure, defects in HCP metals and alloys have a number of features that is of great interest to them and requires detailed consideration. In an ideal HCP – structure each atom is characterized by 6 sets $[1|4|2|1]$ and 6 sets $[1|4|2|2]$. The ability of metals to form alloys with specific physical and mechanical properties is crucial for the technical application. Because of the strong anisotropy of the structure, defects in HCP metals and alloys have a number of features that is of great interest to them and requires detailed consideration.

Currently, the many-body potentials of the embedded-atom method (EAM) [1,2], Finnis–Sinclair [3] potentials and the second-moment approximation (SMA) of the tight-binding (TB) method [4-9] were studied. According to [4,5], the TB-SMA expression of the total energy of a metallic system is based on a small set of adjustable parameters, which can be determined by adjusting to experimental data [9,10] or ab-initio results [1,10-13]. The author of [12], was studied the features of structural transformations of HCP metallic Ti nanowires using Cleri-Rosato potential at low temperature. In [13-17] the mechanical properties of Ni nanowires were studied in detail. There were other representations [18-20].

Thus, the present work, with the assistance of molecular dynamics simulation (Cleri-Rosato potential), structural-energy transformations in HCP Metallic (Cd, Co, Mg, Ti, and Zr) nanowires, under high-speed deformation of uniaxial tension been processed using mathematical modeling. To the study structural-energy transformations, under high-speed of deformation (10^{10} s^{-1}) were applied on pure metallic nanowire (Cd, Co, Mg, Ti, and Zr). This material has a positive temperature dependence of yield stress. The deformation in such alloys can be a combination of structural and superstructural changes, which entails various effects.

Finally this article discusses the results of Molecular Dynamics simulation to HCP phase in metallic nanowires, obtained using the interatomic potential of strong coupling (tight-binding).

2. MD simulation methodology

MD is a simulation technique where the time evolution of an interacting atoms is followed by integrating their equation of motion. It consists of integrating Newton's second law for each atom present in the system by discretization of time. In general, it is difficult to obtain an analytical solution that precisely describes the atoms' trajectories. Therefore, the equations of motion are solved numerically using a time-discretized finite difference methodology such as the Verlet method or the velocity Verlet method, which incorporate the velocities explicitly into the integration scheme. The initial atomic positions for metallic systems are defined on the crystal lattice of the metal, while the initial velocities are assigned according to the Boltzmann distribution at the given simulation temperature. The validity and accuracy of MD simulation results depend on the accuracy of the interatomic forces used as inputs, which rely on the selection of an efficient underlying interatomic force-field potential. For modeling metallic systems, the most

Modeling considered atomic systems was carried out in the framework of multiparticle tight-binding potential Cleri-Rosato. The repulsive part of this potential is short-range repulsive pair potential Born-Mayer and the attractive part arises from the so-called tight-binding (TB) method second-moment approximation to the electronic density of state in which the ion-ion interaction is described by the band terminology [6]. The uses of these

potentials are well established in a number of studies [7-10]. This potential has been used in several studies of bulk and cluster systems transition and noble metals [1,6-7,13].

Commonly used potential is the semi-empirical embedded atom method (EAM) potential. The parameters of EAM potential are generally obtained by fitting cohesive energy, equilibrium lattice constant, elastic constants, unrelaxed vacancy formation energy, bond length, and diatomic bond strength. Since its introduction, the ability and viability of EAM in modeling metals have been extensively analyzed and tested. The classic EAM method is not suitable for describing systems in which covalent bonds are present, such as carbon (in diamond or graphite structures), because the EAM description does not account for the angular dependence of the interatomic interactions. To account for angular dependence, as in the case of the HCP lattice where it is important, a modified embedded atom method was proposed. The total energy U in a system of N atoms in the EAM framework can be written as:

$$U_s = \sum_i (E_i^R + E_i^B), \quad (1)$$

where

$$E_i^R = \sum_{j \neq i} U_{ij}(r_{ij}) = \sum_j A \cdot \exp[-p(\frac{r_{ij}}{r_0} - 1)], \quad (2)$$

is the two-body term, and

$$E_i^B = -\sqrt{\sum_{j \neq i} \varphi(r_{ij})}, \quad (3)$$

$$\varphi(r_{ij}) = \zeta^2 \cdot \exp[2q(\frac{r_{ij}}{r_0} - 1)], \quad (4)$$

is the many-body term. Where A , p , q , ζ , r_0 - are adjustable parameters governing the interaction between those atoms, r_{ij} - the separation between atoms i and j . The values of Potential parameters Cleri-Rosato were taken from [21]. Table 1 gives the parameters of tight-binding potentials for HCP metals used in this work [21].

Table 1. Parameters of tight-binding potentials for HCP metals [21]

	A (eV)	ζ (eV)	p	q	β
Cd	0.1420	0.8117	10.612	5.206	1.8856
Co	0.0950	1.4980	11.604	2.286	1.6232
Mg	0.0290	0.4992	12.820	2.257	1.6335
Ti	0.1519	1.8112	8.620	2.390	1.587
Zr	0.1934	2.2792	8.250	2.249	1.5925

The model can be used to describe quite well elastic, plastic, defect and mechanical properties of a wide range of FCC- and HCP-metals. Verlet algorithm used to determine the velocities of atomic motion in the simulation were. Cleri-Rosato potentials which were proposed by [21] have already worked well in HCP nanowires studies.

The use of such a cutoff radius ensures that the calculations will not consume large amounts of computational time in evaluating the forces that are near zero. The MD simulations require the solution of $6N$ (N -total number of atoms) simultaneous, coupled, first-order differential equations of motion. This solution is obtained using a fourth-order Runge-Kutta algorithm. Integration accuracy is monitored using back-integration and energy conservation requirements with the velocity reset procedure turned off. The MD simulations were carried out till separation occurs in the tensile specimen.

3. Results and discussion

Since the deformation and fracture of HCP nanowires are of main interest in this work (Table 2). The specimen used for the studied section is a nanowire of $12a_0 \times 12a_0 \times 12c_0$. The total number of atoms used in the simulations equal 1928 according on the crystal structure. The crystal was set-up with a hexagonal orientation and the uniaxial tensile force was applied along the [0001] direction. The feature of deformation, slipping, twinning and necking were studied.

Table 2 gives the measured tensile strength and strain to fracture of the various materials used in this work. As can be expected, Zr exhibits the highest strength (yield strength of =23GPa) while Mg exhibits the lowest strength (yield strength of =4GPa). The strength of Ti was estimated to be=14GPa. The strength of Co was estimated to be =22.5GPa. The strength of Cd was estimated to be =6 GPa. Cadmium showed an earlier fracture while Cobaltshowed the maximum strain before fracture.

Table 2. MD results for calculating of HCP nanowires at 300 K including yielding time, yielding stress and breaking time

HCP Nanowire	Yielding point		Breaking time
	σ (GPa)	T, Ps	t , Ps
Cd	6	10	135
Co	22.5	8	170
Mg	4	8	140
Ti	14	4	150
Zr	23	4	140

Three stages deformation. The experiments were obtained plots of the stored energy of deformation at various times, reflecting the processes in the HCP nanowires during deformation. There are three stages of deformation: the quasi-elastic deformation (I), plastic deformation (II) and the breaking (failure) (III).

For all HCP nanowires, in the first stage there was almost linear increase in stress. The initial stage quasi-elastic area there is only relative displacement of atoms and there are no defects. Therefore, in this region the energy stored varies periodically. This stage is completed at 8 Ps, 8 Ps, 4 Ps, 4 Ps for Mg, Co, Ti and Zr nanowires, respectively. The sharp fall takes place only at the point of transition from the first to second stages of deformation (Fig. 1).

Analysis of the graphs in Fig. 1 shows that the average duration of the first stage of deformation for nanowire, The duration of the plastic deformation step is 210, 160, 165, 115 Ps, for Mg, Co, Ti and Zr nanowires, respectively.

The value of the stored energy at the peak of deformation schedule at the end of the first stage for the reduced nanowires equals 0.05, 0.07, 0.05 and 0.045 eV / atom, respectively. The levels of stored energy at the end of the plastic deformation steps are equals 0.065, 0.145, 0.115, and 0.112 eV / atom, respectively. The neck of the HCP nanowire forms after the slips happened, and the deformations have been carried mainly through the elongation of the neck. Through further analysis, we find that the last stage of plastic deformation of the neck is formed; deformation develops mainly due to the reconstruction and rebuilding of the neck area. Outside this area, the HCP nanowires ordered structure is retained and there are significant changes. Beyond the neck region, atomic structures have no significant changes. The atomic rearrangements in the neck region induce the zigzag increase–decrease in stress as the strain is increased. The atoms, close to the narrowest region of the neck, are highly disordered.

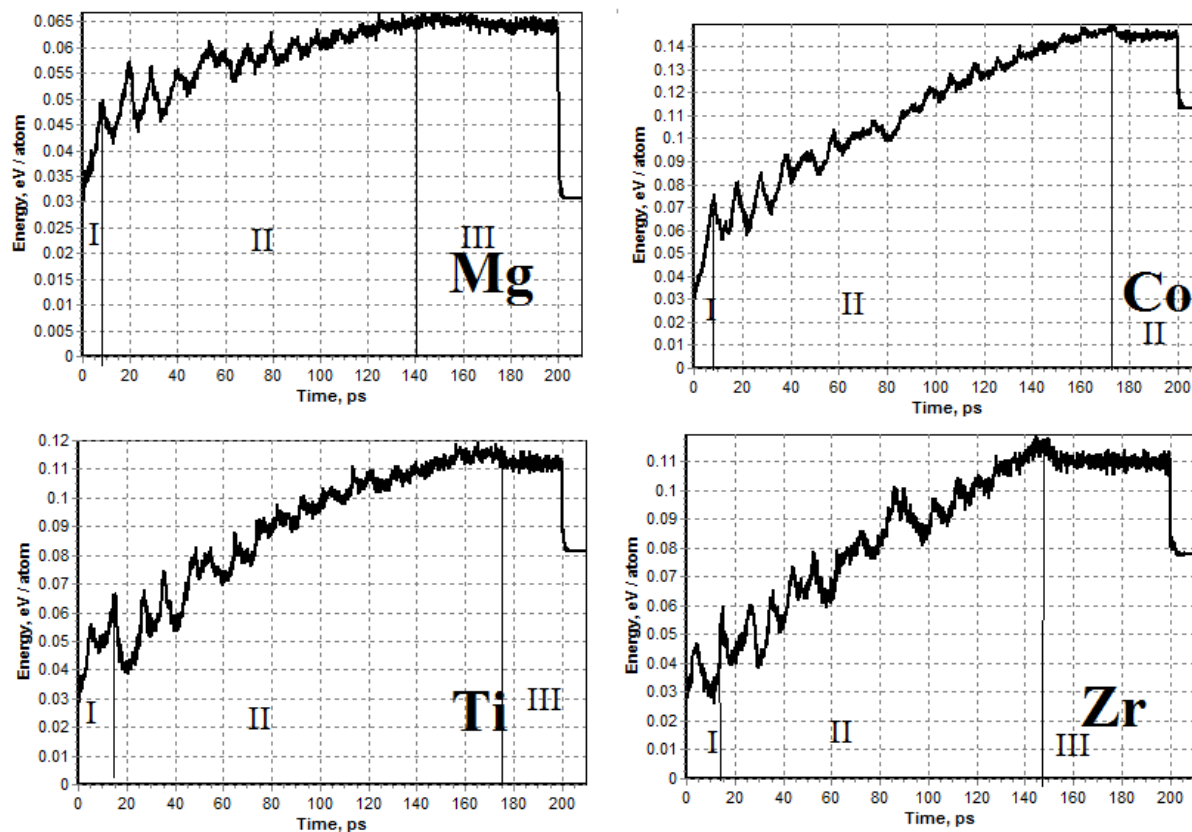


Fig. 1. The dependence of the energy stored by the deformation time of the experiment at 300 K at various time of uniaxial loading for Mg, Co, Ti and Zr nanowires

At the point of breaking, we observe a one-atom thick. With further pulling of the HCP nanowires, the bond between the two atoms lying in the one-atom breaks and then the rupture happens. As can be expected Zirconium exhibits the highest ultimate strength (≈ 26 GPa), while the ultimate strength of Titanium nanowire was estimated to be 18 GPa.

Structure transformation of HCP metallic nanowire. The MD simulation plots of the XOY plane of the tensile specimens at various stages of uniaxial tension are shown in Figs. 2-5 are for the HCP materials, Cd, Co, Mg, Ti and Zr, respectively, It may be noted that the discussion of the results presented here is based not only on the MD simulation plots of the various stages presented here but also on the detailed study of the animation of the process [12].

Figure 6 shows a small compressive bulge of the specimen after the relaxation at time 4 Ps for Zr. A similar situation is found for the other HCP metals investigated, namely, Cd, Co, Mg and Ti. Considerable disorder in the XOY plane of the crystal was observed during the early stages of deformation for all HCP metals (up to 50 Ps as in Figs. 2-5).

As the HCP nanowires was extended, necking area can be seen at times 135 Ps, 170 Ps, 150 Ps, 140 Ps for Cd, Co, Mg and Zr nanowires, respectively, (Figs. 2-5). Since Co is a highly ductile material, the atoms hold together under larger strain before the dislocations formed during the elastic and plastic deformation dislocation and form a ductile fracture. Towards the end of plastic deformation, the neck is elongated almost linearly to a very large strain (Fig. 2). On subsequent pulling, the necked region separates in the failure at 170 Ps.

The radius of the neck was found to increase with increase in the deformation of the nanowire and to decrease with decrease in the ductility. Thus, the radius decreases as we go from Co to Zr to Co to Mg. The region of disordered material as well as the extent of vacancy formation was also found to decrease with decrease in the ductility of the wire.

Initially, dislocations at $\approx 35^\circ$ were observed in the MD data for the case of Zr but due to the high disorder, further dislocation propagation can be observed. Based on the results, as well as the MD simulations at first stage of deformation (Figs. 2-5), the strain to fracture was observed to the HCP nanowires. This can be observed by comparing Figs. 2-5 which shows the variations in the strain to fracture of various nanowires. In the case of HCP nanowires, the work material was disordered from the early stages of necking till the end of the experiment.

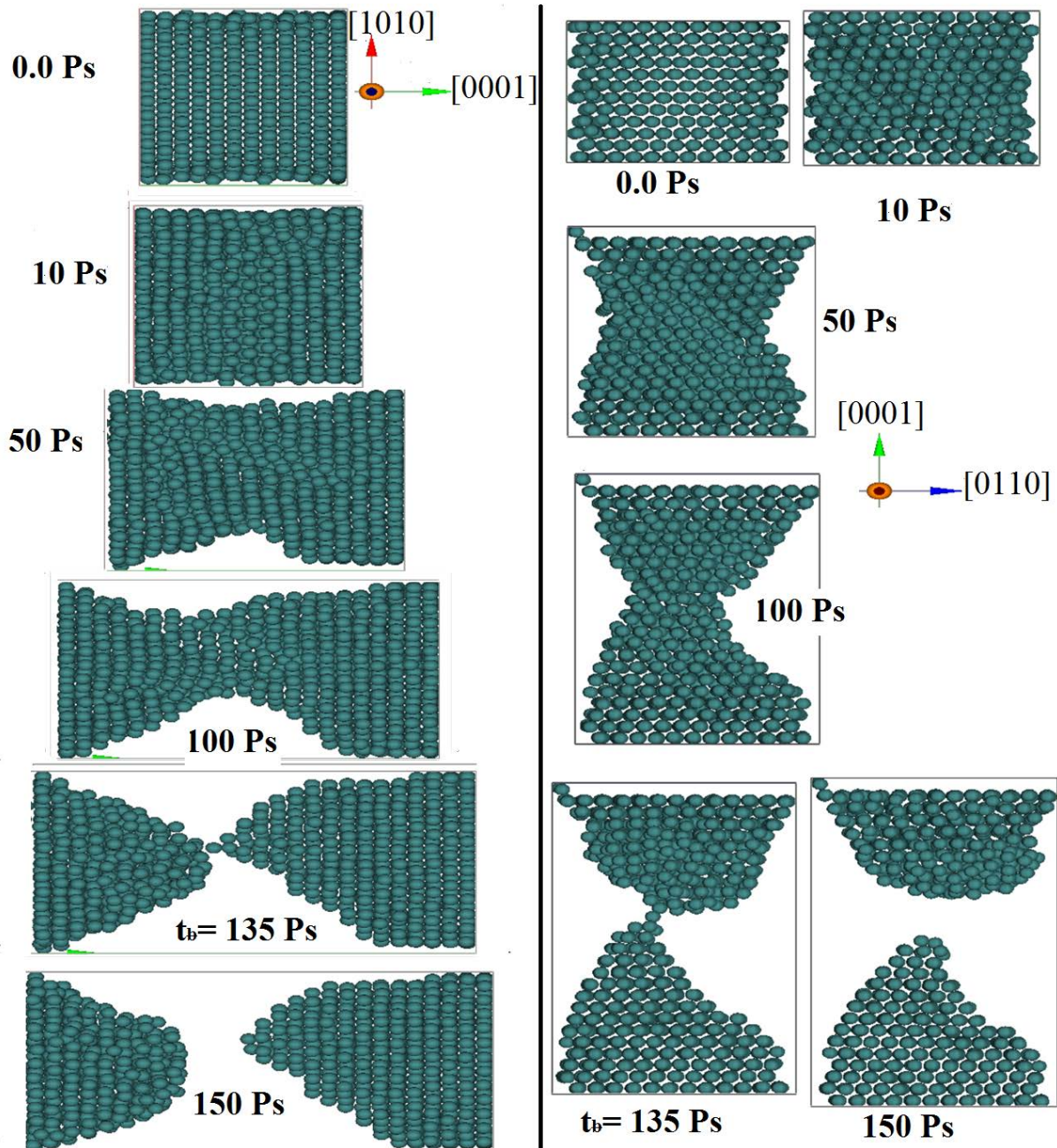


Fig. 2. MD simulation plots of the gage section of a tensile specimen at various time of uniaxial loading for Cd nano-wire in plane [1010] right and in plane [0110] left

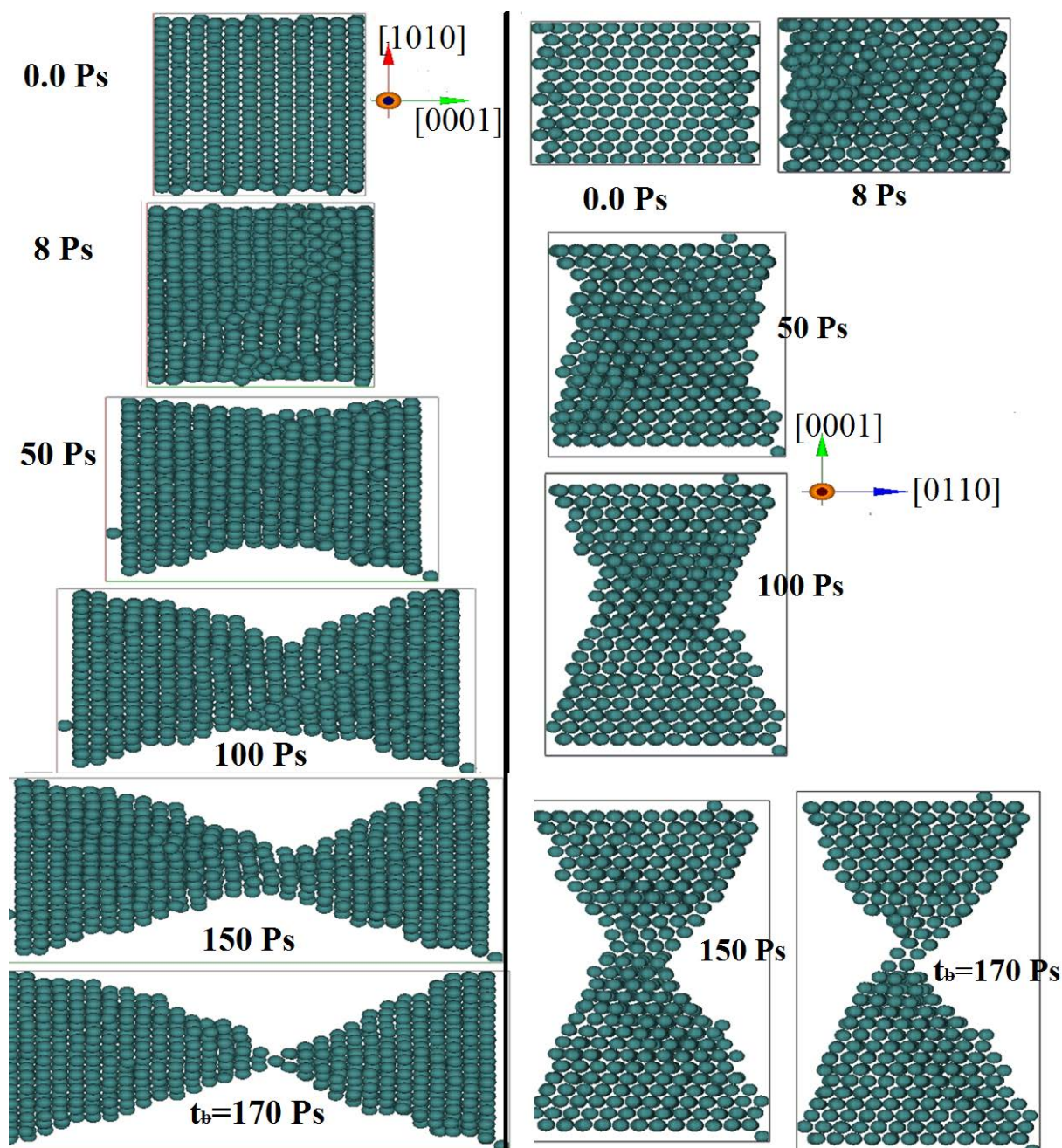


Fig. 3. MD simulation plots of the gage section of a tensile specimen at various time of uniaxial loading for Co nanowire in plane $[1010]$ right and in plane $[0110]$ left

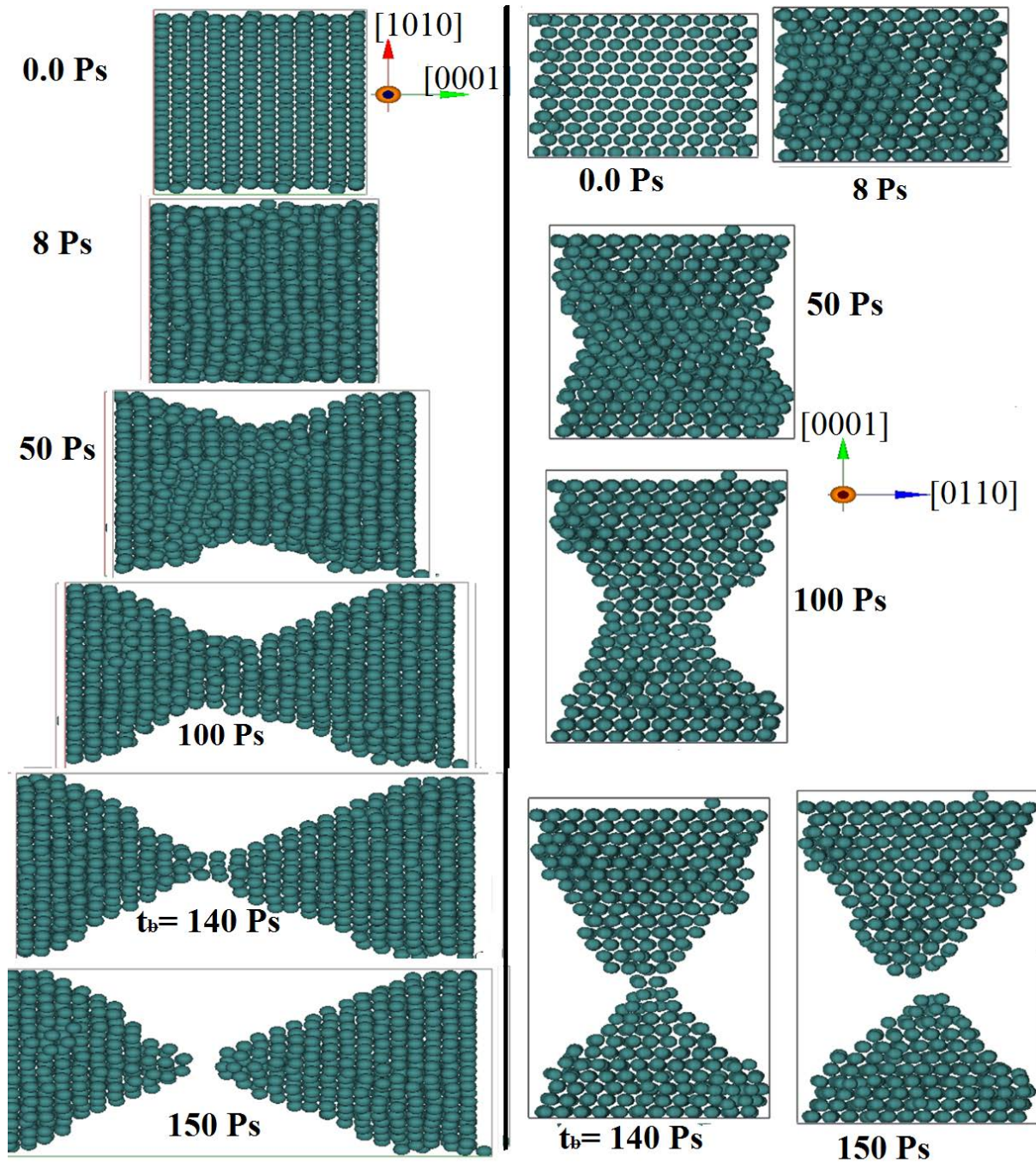


Fig. 4. MD simulation plots of the gage section of a tensile specimen at various time of uniaxial loading for Mg nanowire in plane $[1010]$ right and in plane $[0110]$ left

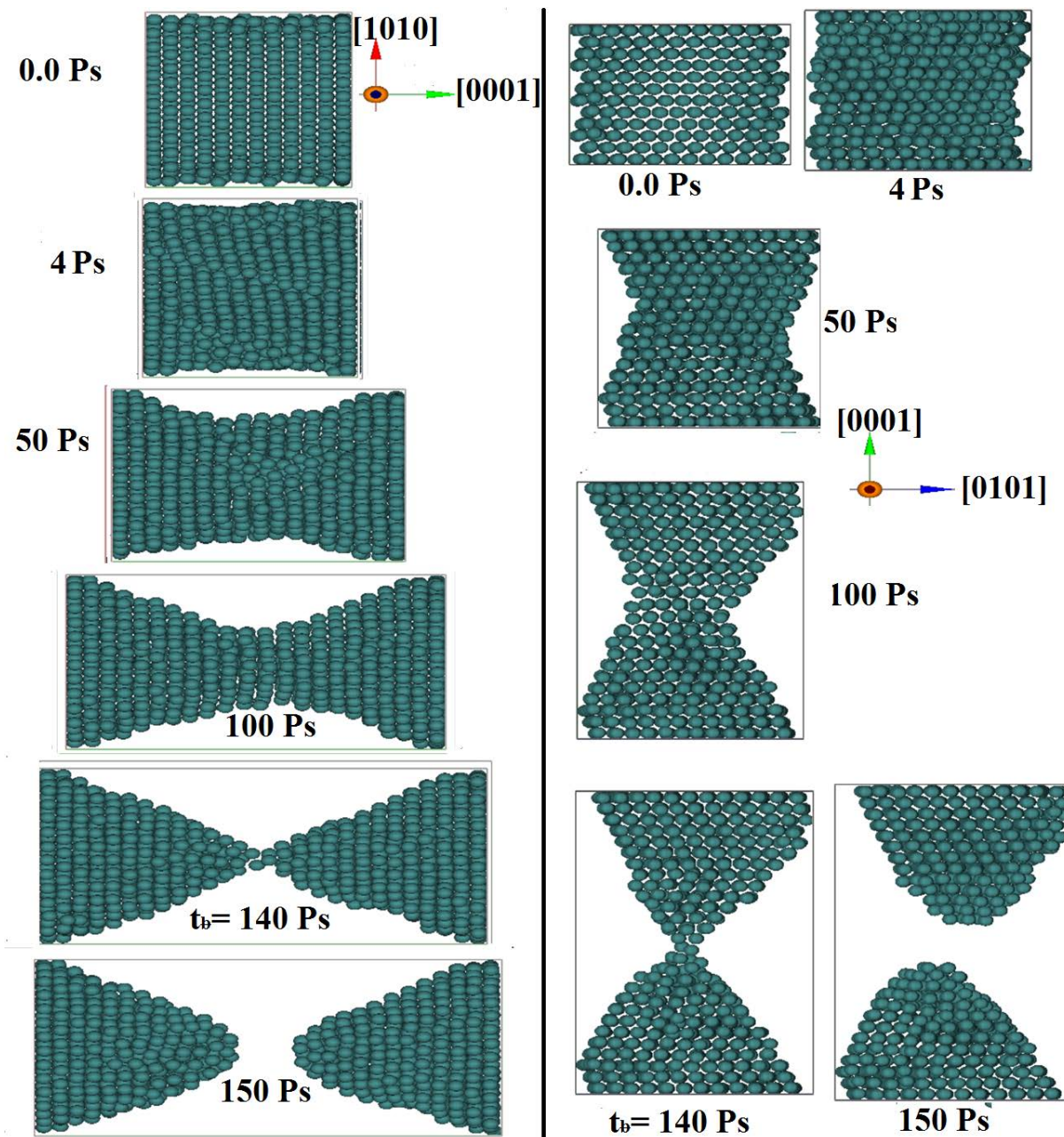


Fig. 5. MD simulation plots of the gage section of a tensile specimen at various time of uniaxial loading for Zr nanowire in plane $[1010]$ right and in plane $[0110]$ left

4. Conclusions

The process of formation of defects in the dynamic deformation of HCP metallic (Cd, Co, Mg, Ti, and Zr) nanowires under uniaxial tension at 300 K have been studied using MD simulation. Structural differences between the structural and energy transformations were as follows: As a result of studies of structural and energy transformations during tensile deformation of HCP metallic (Cd, Co, Mg, Ti, and Zr) nanowires at 300 K, identified three stages of structural and energy transformations: the quasi-elastic, plastic(flow), and fracture.

1. The first stage of structural and energy transformations in the deformation process ends with formation sliding on the substructure of HCP metallic (Cd, Co, Mg, Ti, and Zr) nanowires. At the first stage of deformation, we can see rotation the central portion of nanowire and C-domain formation in the second stage of deformation. The first stage of

structural and energy transformations ends quickly for all of them and peak values 4 Ps for Ti and Zr, 8 Ps for Co and Mg and 10 Ps for Cd. As can be expected the ultimate strength of the HCP nanowires equals 23, 22.5, 14, 6 and 4 for Zr, Co, Ti, Cd and Mg nanowires, respectively,

2. It was found that the features of structural and energy transformations for HCP metallic nanowires in the second stage of deformation affects the orientation of the axis of tension. In the second stage occur collective atomic bias, the formation of dislocations and grain boundaries. As shown in Fig. 2 the period of the plasticity was tacked largest period of time for Co and Ti and smallest for Zr and Mg.

3. The value of the stored energy at the peak of deformation schedule at the end of the first stage for the reduced nanowires equals 0.07 eV/atom for Co and 0.045 eV/atom for Zr. The levels of stored energy at the end of the plastic deformation steps are equals 0.065 eV /atom for Mg and 0.112 eV /atom for Zr.

4. The neck area occurs in the third stage of structural and energy transformations. Stored strain energy in that period varies only slightly.

5. The nature of the destruction of blocks corresponds to brittle fracture at 300 K. After fracture of nanowire for all nanowires, found planar defects such as twins and packing defects.

Acknowledgements. No external funding was received for this study.

References

- [1] Liang T, Phillpot SR, Sinnott SB. Parameterization of a reactive many-body potential for Mo–S systems. *Phys. Rev. B.* 2009;79(24): 245110.
- [2] Mishin Y, Farkas D, Mehl MJ, Papaconstantopoulos DA. Interatomic potentials for monoatomic metals from experimental data and ab initio calculations. *Phys. Rev. B.* 1999;59(5): 3393.
- [3] Mishin Y, Mehl MJ, Papaconstantopoulos DA, Voter AF, Kress JD. Structural stability and lattice defects in copper: Ab initio, tight-binding, and embedded-atom calculations. *Phys. Rev. B.* 2001;63(22): 224106.
- [4] Mishin Y, Mehl MJ, Papaconstantopoulos DA. Embedded-atom potential for B₂NiAl. *Phys. Rev. B.* 2002;65(22): 224114.
- [5] Zope RR, Mishin Y. Interatomic potentials for atomistic simulations of the Ti–Al system. *Phys. Rev. B.* 2003;68(2): 024102.
- [6] Elstner M, Porezag D, Jungnickel G, Elsner J, Haugk M, Frauenheim T, Suhai S, Seifert G. Self-consistent-charge density-functional tight-binding method for simulations of complex materials properties. *Phys. Rev. B.* 1998;58(11): 7260.
- [7] Mishin Y, Mehl MJ, Papaconstantopoulos DA. Phase stability in the Fe–Ni system: Investigation by first-principles calculations and atomistic simulations. *Acta Mater.* 2005;53(15): 4029.
- [8] Ghosh G, Delsante S, Borzone G, Asta M, Ferro R. Phase stability and cohesive properties of Ti–Zn intermetallics: First-principles calculations and experimental results. *Acta Mater.* 2006;54(19): 4977–4997.
- [9] Chamati H, Papanicolaou N, Mishin Y, Papaconstantopoulos DA. Embedded-atom potential for Fe and its application to self-diffusion on Fe (100). *Surf. Sci.* 2006;600(9): 1793–1803.
- [10] Robertson IJ, Heine V, Payne MC. Cohesion in aluminum systems: A first-principles assessment of "glue" schemes. *Phys. Rev. Lett.* 1993;70(13): 1944.
- [11] Frederiksen SL, Jacobsen KW, Brown KS, Sethna JP. Bayesian Ensemble Approach to Error Estimation of Interatomic Potentials. *Phys. Rev. Lett.* 2004;93(16): 165501.
- [12] Aish MM, Starostenkov MD. Features of structural transformations of HCP metallic Ti

- nanowires using Cleri-Rosato potential at low temperature. *Letters on Materials*. 2016;6(4): 317-321.
- [13] Starostenkov MD, Aish MM. Feature deformation and breaking of Ni nanowire. *Letters on Materials*. 2014;4(2): 89-92.
- [14] Aish MM, Starostenkov MD. Deformation and Fracture of Metallic Nanowires. *Solid State Phenomena*. 2017;258: 277-280.
- [15] Aish Mohammed, Starostenkov Mikhail. Mechanical properties of metallic nanowires using tight-binding model. *AIP Conf. Proc.* 2016;1698: 040006.
- [16] Aish MM, Starostenkov MD. Characterization of strain-induced structural transformations in CdSe nanowires using molecular dynamics simulation. *Materials Physics and Mechanics*. 2015;24(4): 139-144.
- [17] Starostenkov MD, Aish MM. Molecular dynamic study for ultrathin Nickel nanowires at the same temperature. *Materials Physics and Mechanics*. 2014;21(1): 1-7.
- [18] Starostenkov MD, Aish MM. Effect of length and cross-sectional area on Ni₃Fe alloy plasticity. *Advanced Materials Research*. 2014;1013: 242-248.
- [19] Aish MM, Starostenkov MD. Effect of volume on the mechanical properties of nickel nanowire. *Materials Physics and Mechanics*. 2013;18(1): 53-62.
- [20] Aish MM. The Structural Transformation and Mechanical Strength of Ni, Ti Nanowires and Nitinol Alloys at Various Vacancy Rates: Molecular Dynamic Study Using Cleri-Rosato Potential. *Materials Physics and Mechanics*. 2019;42(2): 211-223.
- [21] Cleri F, Rosato V. Tight-binding potentials for transition metals and alloys. *Phys. Rev. B*. 1993;48(1): 22.